Proceedings of the 2021 IEEE
International Conference on Robotics and Biomimetics
December 27-31, 2021, Sanya, China

2021 IEEE International Conference on Robotics and Biomimetics (ROBIO) | 978-1-6654-0535-5/21/$31.00 ©2021 IEEE | DOI: 10.1109/ROBIO54168.2021.9739274

Putty Plastering Realized by a Force Controlled Robotic Scraper

[1]Zhao Liu, [1]Dayuan Chen, [1]Xin Jiang* and [2]Yunhui Liu

***Abstract*— Research on construction robotics has attracted increasing attention as the rising labor costs become prominent. Compliance control, including impedance/admittance control, is considered as a classical approach for robotic manipulation tasks involving contact. In this paper, we propose a putty plastering strategy based on a force controlled scraper which is mounted at the end-effector of an interior finishing robot. In order to control the quality of putty plastering, we verified several strategy including active parameters adjustment of impedance control, active adjustment of scraper speed/tilt angle. The plastering experiments in a construction site proved that the proposed plastering strategy is effective. The evenness and coated putty thickness can meet the quality requirements.**

I. Introduction

Due to the harsh environment of construction sites and the frequent occurrence of safety accidents during operations, young laborers are gradually leaving the construction industry, which leads to the aging of workers and higher labor costs. For this reason, the research of construction robots has attracted more and more attention.

In 2007, two decoration robots for wall painting were developed by the Polytechnic University of Marche, Italy [1]. One was for low-rise wall painting, and the other was attached to the wall for high-rise wall painting. After this project, the development of construction robots was accelerated. Robots for bricklaying [2] was developed at ETH. Tiling robots were developed at Harvard University [3]. NTU developed a semi-autonomous robot Pictobot [4] for spraying walls, and QuicaBot [5], a fully automated robot for interior decoration quality inspection.

Some of the robots are for tasks involving non-contact with environment, like painting and quality inspection robots, and some are designed for tasks involving contact, like wall sanding and tiling. The contact considered by most of construction robots are rigid ones, which have high stiffness and stationary state. For fluid material like putty, its shape, viscosity, and stiffness will change with applied force and time. It is difficult to ensure the evenness of the plastered putty by simple operation and control.

To solve the problem, Li et al [6] proposed a robot end-tool with spring suspension and combined it with a neural network to achieve automatic putty plastering. Du et al [7] proposed a path planning approach to optimize the trajectory of a robot if it needs to apply a putty applying operation to a large scale room. The method adopted in [6] has poor adaptability to complex environments for passive compliance achieved by the spring suspension. In the experiments, after each plastering operation, a new footprint is left. To overcome the drawbacks of passive compliance, active force control [8] [9] have been proposed for tasks involving contact with environment. Among the methods, impedance control is widely applied. This method has strong robustness and requires low positional accuracy between the end-effector and the environment, which is suitable for construction site scenarios.

In this article, we imitate the manual operation of lateral plastering based on the impedance control realized by a force controlled scraper and we switch among 3 impedance coefficients according to the state of the putty respectively. At the boundaries of two operation areas, we actively adjust the robot arm operation height and the scraper tilt angle, which can effectively reduce the lateral stripes left on the plastered surface after operations. After the mobile chassis drives to the next station, we propose the active adjustment of the scraper's tangential speed to reduce footprint produced by the scraper. With the above strategies, it is proved that the surface evenness and thickness of the putty met the quality requirements.

This paper is organized as follows: Section II briefly introduces the robot platform used. Section III introduces the plastering strategy used in operations.

Corresponding author: Xin Jiang(*x.jiang@ieee.org*)

[1]Zhao Liu, Dayuan Chen and Xin Jiang are with School of Mechanical Engineering and Automation, Harbin Institute of Technology, Shenzhen, HIT Campus Shenzhen University Town, Xili, Shenzhen, 518055, China.

[2]Yunhui Liu is with the Department of Mechanical Engineering,The Chinese University of Hong Kong, Hong Kong, China *yhliu@mae.cuhk.edu.hk*

Section IV shows the experiment and results. Finally, conclusions are presented in Section V.

II. The Robot Platform for Putty Plastering

A. The robot platform

As shown in Fig. 1, the putty plastering robot is mainly composed of a mobile chassis, a lifting platform, a 6 DOFs UR5 robot arm, a 3 DOFs parallel platform, and a specially designed end-effector for putty plastering. To realize the communication among the robot components, we use the ROS as the control center. The specific communication logic is shown in Fig. 2.

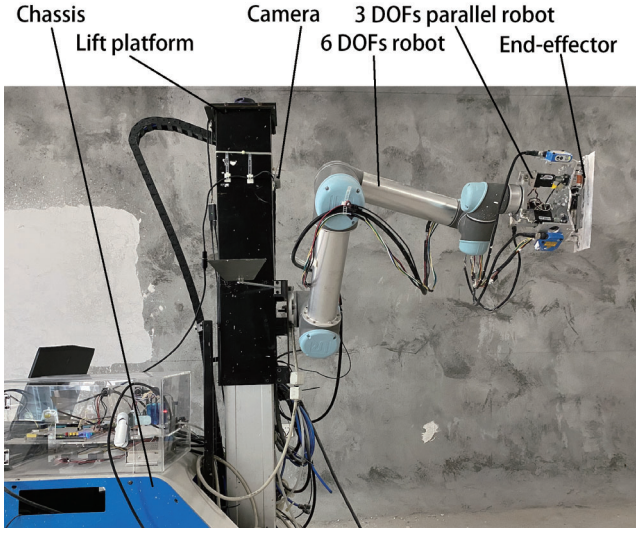

Fig. 1. Robot platform

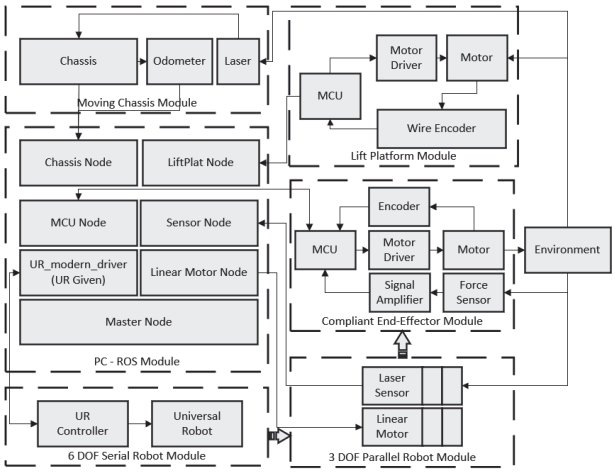

Fig. 2. Robot system framework

The 3-RPS parallel platform is controlled by 3 linear motors with a maximum servo frequency of 200 Hz, which is higher than the UR5 frequency 125 Hz.

The UR5 robot arm is connected in serial style with the parallel platform which results in a micro/macro manipulator with a total of 9 DOFs. We define the speed of this robot

$$\dot{x} = J\dot{\theta} \tag{1}$$

where J is a 6×9 Jacobian matrix, $\dot{\theta}$ is a 9×1 vector summarizing the angular velocity of each joint, and $\dot{x}$ is a 6×1 vector representing the linear and angular velocities in Cartesian space. We need to solve J to obtain the relationship between the input joint velocity and the output end-effector motion velocity.

$$J = \begin{bmatrix} J_M & J_m \end{bmatrix} \tag{2}$$

J_M is the Jacobian matrix of UR5 with the parallel platform motion chain and J_m is the parallel platform Jacobian matrix after the rotation from the end of the UR5 to the world coordinate system.

$$J_m = \begin{bmatrix} {}^{W}_{5}R & 0 \\ 0 & {}^{W}_{5}R \end{bmatrix} J_{RPS} \tag{3}$$

Where ${}^{W}_{5}R$ represents the rotation matrix of the UR5 from the world coordinate system to the 6 joints. J_{RPS} is the parallel platform Jacobian matrix. We will obtain the relationship between the speed of each joint and the end-effector speed by solving J_{RPS}. Please check [10] for a detailed derivation.

B. The parallel platform and end-effector

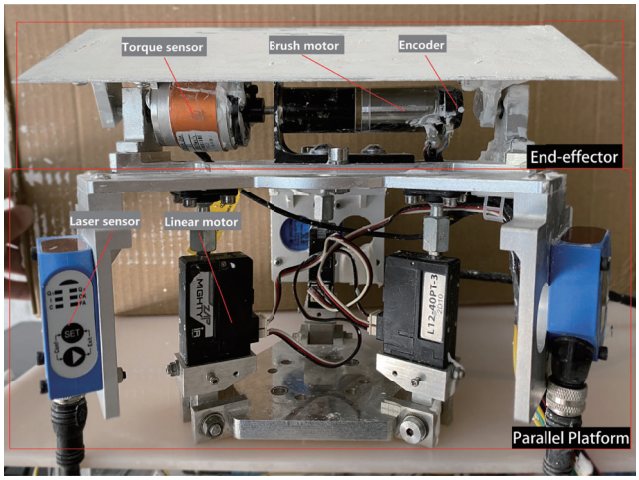

Fig. 3. Parallel platform and end-effector

As shown in Fig. 3, the parallel platform can achieve 1 DOF of translational motion and 2 DOFs of rotation. Laser sensors are applied to adjust the pose of the end-effector to the wall. The end-effector

consists of one-dimensional torque sensor, a DC brushed motor, and an incremental angle encoder.

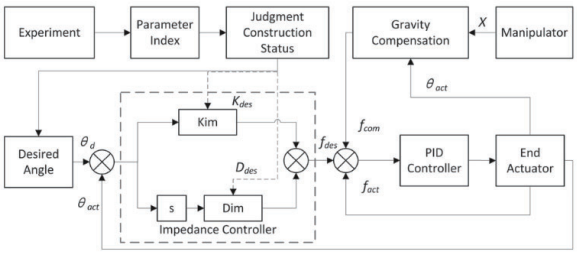

Fig. 4. Structure of the impedance control

We use the classical impedance control method, as shown in Fig. 4

$$f_{im} = K_{im}(\theta_{des} - \theta_{act}) + D_{im}(\dot{\theta}_{des} - \dot{\theta}_{act}) \quad (4)$$

K_{im} is the stiffness coefficient, D_{im} is the damping coefficient, θ_{des} is the desired angle, θ_{act} is the actual angle of rotation, and f_{im} is the torque measured from torque sensor.

III. The Plastering Strategy

A. Workflow

The plastering robot operation is divided into 3 processes.

1) Preparation stage. UR servo to achieve coarse positioning, and use the laser sensor to measure the distance from the wall for fine positioning. At the same time the robot adjusts the parallel platform attitude to make the scraper plane maintain the presetting angle with respect to the wall.

2) Plastering putty stage. In this stage, we implement a lateral plastering operation taking reference to similar operation done by human worker. To remove the scratches produced by every two transverse scrapings, as shown in Fig. 5, we actively adjusted the tilt angle so that the scratches can be thinned.

3) Stage transition between two sequential stations. When the chassis moves to the next station, the end of the previous station and the start of new station needs to be smoothly transitioned. Then stage 1) 2) will be repeated.

B. Selection of impedance coefficient

From [10], it can be seen that the impedance controller of the end-effector can change its own compliance by changing its stiffness coefficient under the same external forces. The experimental results show that the smaller the stiffness coefficient is, the softer the contact to the wall will be. Based on previous experimental results [10], we chose the parameters shown in Table I for the experiment and verified them in Section IV.

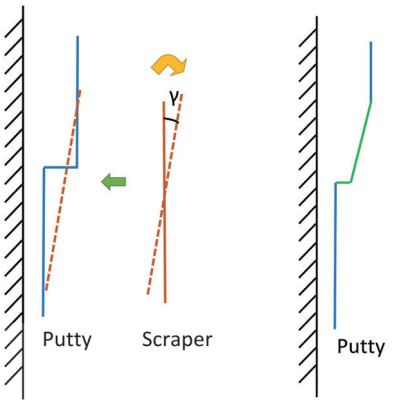

(a) Adjusted the tilt angle (b) Result

Fig. 5. Adjusted the tilt angle and result

TABLE I
IMPEDANCE COEFFICIENT SELECTION

Category	Stiffness coefficient	Damping coefficient
Soft	5	0.2
Standard	20	0.1
Hard	50	0.1

C. Treatment to vertical stripes between two successive stations

As shown in Fig. 6, 7, when the chassis moves to the next station, the scraper rotates and makes contact with the putty. It produces a distinct longitudinal stripe. For this reason, we propose 3 solutions.

1) Feedback the detected torque to position control, i.e., we can obtain the torque when the scraper touches the putty during the rotation. Therefore, we can assume that if the scraper senses contact it stops rotating until lateral plastering begins.

2) Dynamic adjustment of the impedance coefficient, i.e., in the initial state, a small impedance coefficient is set, and the scraper bounces back after contacting the putty with the torque obtained during this process, we can gradually increase the impedance coefficient to the target value when plastering laterally.

3) Active increase of the tangential speed of the scraper, i.e. UR arm will move with the rotation of the scraper to increase the radius of curvature generated at the contact.

The above solutions will be described in Section IV to demonstrate the experimental process and results.

Fig. 6. Vertical stripes defects

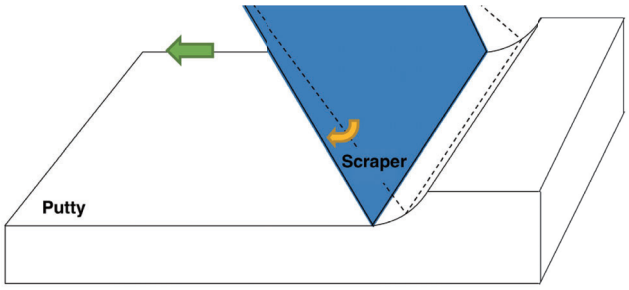

Fig. 7. Stripes diagram

IV. Experiments and Results

A. Experiments with variable impedance coefficients

Different impedance coefficients should be used separately according to the the status of the plastered putty, as shown in Fig. 8. In the experiment, the robot deals with a putty block 15 *cm* from the center of the working space. We used 3 different groups of impedance coefficients shown in Table I for the plastering and observed the surface status of the putty, as shown in Fig. 8(c). It can be seen that there is an obvious difference between the putty surfaces after treatments with different impedance coefficients in Table II.

TABLE II
Analysis of Treated Putty Surface 1

Dealing coefficient	Surface analyse
Soft	Obvious steps at the top and bottom edges, obvious holes in the middle, some longitudinal stripes at the end
Standard	A little kernel, a little vertical stripe
Hard	No particulate matter, a few longitudinal stripes

The "hard" coefficient is the best for this situation. For further observation, we investigate the relationship between the distance from the scraper blade to the wall.

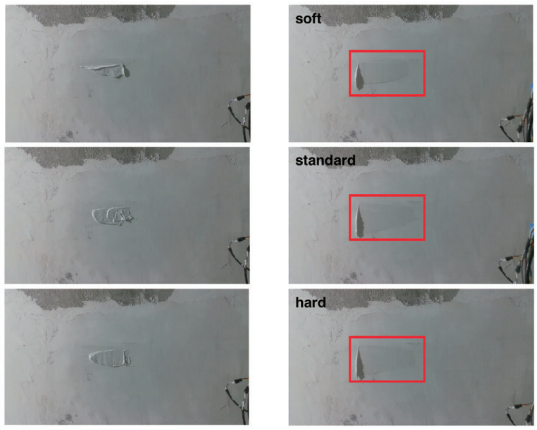

(a) Before plastering (b) After plastering

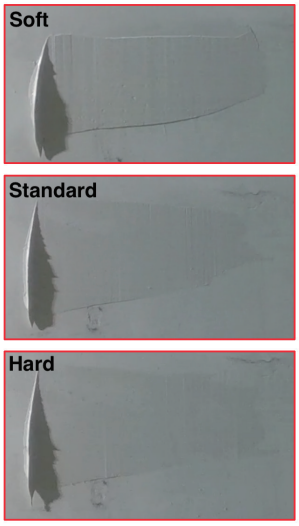

(c) Enlarge

Fig. 8. Impedance experiment 1

$$d_{2wall} = d_{laser} - d_{tool} \tag{5}$$

Where d_{tool} is the distance from the scraper blade to the head of the laser sensor, d_{laser} is the distance from the surface of the putty to the head of the laser sensor, d_{2wall} is the scraping depth into the putty.

As can be seen in Fig. 9, the 3 sets of impedance coefficients lead to different depths of scraper blade into the putty, which generates different status on the plastered putty surface. For this reason, we did more experiments to verify. We applied similar sized blocks of putty to the same area with different stiffness of the base putty. Then, we operated with 3 different impedance coefficients. As shown in Fig. 10(a), "soft" coefficient did not scrape a new footprint with a low stiffness of the base putty. Not only did the "standard"

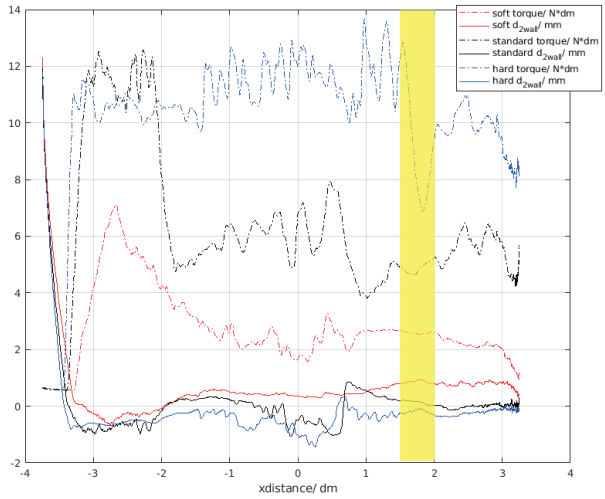

Fig. 9. The x coordinate is the lateral movement position of the end-effector, the dashed line is the measured torque value, the solid line is ${}^{*}d_{2wall}$, and the yellow area indicates the location of the putty block
${}^{*}d_{2wall}$ is calculated from the parallel platform and the scraper, which has a small error, and the scraper rotation angle is a relative value, so the ${}^{*}d_{2wall}$ calculation may be less than 0.

coefficient not scrape a new footprint, it smoothed out the putty block steps with a relatively high stiffness of the base putty, as shown in Fig. 10(b).

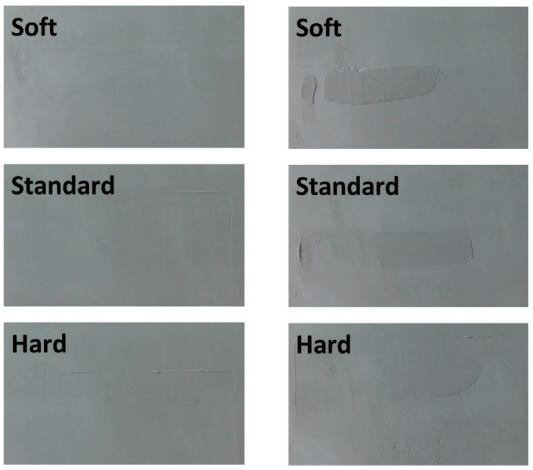

(a) Experiment 2 (b) Experiment 3

Fig. 10. Impedance experiment

These 2 experiments prove that "soft" and "standard" coefficients superiority in some situations, respectively. A proper coefficient can ensure that the plastering motion functions on the upper putty without affecting the base putty layer. Through 3 sets of impedance experiments, we can see that since the state of the putty is related to time, spraying methods, viscosity level, and work progress, it is necessary to use different impedance coefficients to deal with the putty blocks under different conditions to ensure the flatness of the putty.

B. Longitudinal stripe processing experiment

The method proposed in study 1) 2) in *C* Section III requires precise sensing of the contact process between the scraper and the putty, so a layer of putty approximately 1.5 *cm* thick was applied to the wall to test the torque without touching the wall. The relationship between the torque applied to the scraper and the scraper posture was measured, as shown in Fig. 11.

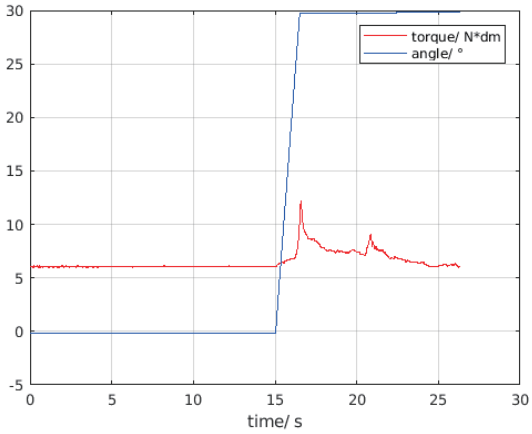

Fig. 11. Torque variation about only contact with putty

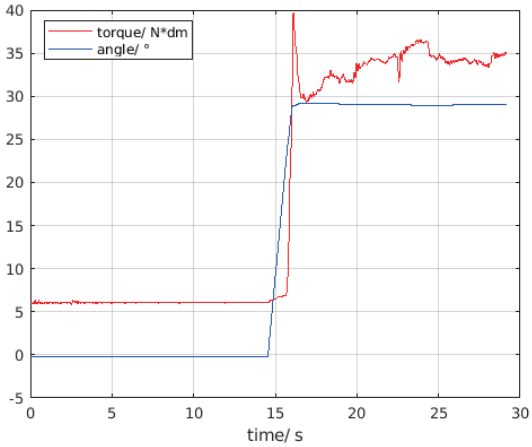

Fig. 12. Torque variation about contact with putty and wall

Fig. 12 shows the torque versus the attitude of the scraper in contact with the wall with thinner putty on surface after rotation, from which we can not detect if the scraper touch the putty or the wall by the data of the torque. There are 2 reasons: one is the machining and assembly errors of the parallel platform, the other

is the problem of tri-laser structure. These reasons cause that we can not ensure the scraper blade is perfectly parallel to the putty surface, which leads to that the upper/lower part of the scraper touch the putty first, touching less of the putty and generating very little viscous force.

Therefore, we used the active method of increasing the tangential speed of the scraper to enlarge the radius of curvature at the transition, as shown in Fig. 7. After several tests, we adjusted the scraper rotation speed and left a surplus of 5 *cm* to ensure that the scraper had a tangential speed before contacting the putty.

Combining the impedance control scheme with the station-station longitudinal stripe treatment strategy, we follow the operation scheme of Section III and scrape the putty plastered in a large region 1.75 $m \times$ 0.48 m as shown in Fig. 13, 14. The result shows that after 3 consecutive plastering operations, no distinct footprints are left.

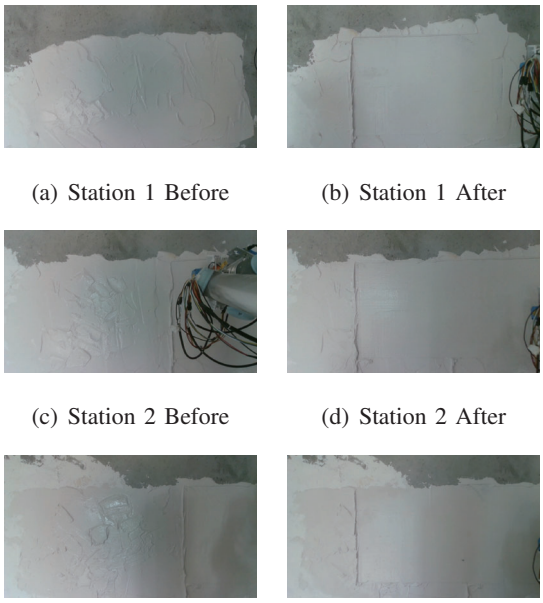

(a) Station 1 Before (b) Station 1 After

(c) Station 2 Before (d) Station 2 After

(e) Station 3 Before (f) Station 3 After

Fig. 13. Overview of the operation

Fig. 14. Experimental results

V. CONCLUSION

In this paper, we propose a putty plastering strategy based on a 3-RPS parallel platform. The method can effectively avoid defects such as stripes and bumps on the putty surface, and after several experimental verification, the superiority of the method is proved, and a wall of 1.75 $m \times$ 0.48 m is plastered with putty by repeatedly applying the proposed strategy. It shows that no distinct defects are left after the operation.

In the near future, we will further expand the operating area of the robot and integrate deep learning networks to determine defective putty treatment solutions in order to achieve a fully automated operation of the plastering robot.

ACKNOWLEDGMENT

This work was supported by the following projects: National Natural Science Foundation of China (Grant No.U1813202), Natural Science Foundation of China (Grant No.61873072), National Natural Science Foundation of China (Grant No.U1713202).

REFERENCES

[1] B. Naticchia, A. Giretti, and A. Carbonari, "Set up of an automated multi-colour system for interior wall painting," vol. 4, no. 4, p. 50.

[2] V. Helm, S. Ercan, F. Gramazio, and M. Kohler, "Mobile robotic fabrication on construction sites: DimRob," in *2012 IEEE/RSJ International Conference on Intelligent Robots and Systems*. IEEE, pp. 4335–4341.

[3] N. King, M. Bechthold, A. Kane, and P. Michalatos, "Robotic tile placement: Tools, techniques and feasibility," vol. 39, pp. 161–166.

[4] E. Asadi, B. Li, and I.-M. Chen, "Pictobot: A cooperative painting robot for interior finishing of industrial developments," vol. 25, no. 2, pp. 82–94.

[5] R.-J. Yan, E. Kayacan, I.-M. Chen, L. K. Tiong, and J. Wu, "QuicaBot: Quality inspection and assessment robot," vol. 16, no. 2, pp. 506–517.

[6] X. Li and X. Jiang, "Development of a robot system for applying putty on plastered walls," in *2018 IEEE International Conference on Mechatronics and Automation (ICMA)*. IEEE, pp. 1417–1422.

[7] Y. Du, X. Jiang, P. Shan, T. Chen, H. Ji, P. Li, C. Lyu, W. Yang, and Y. Liu, "A robotized interior work process planning algorithm based on surface minimum coverage set," in *2017 IEEE International Conference on Robotics and Biomimetics (ROBIO)*. IEEE, pp. 894–899.

[8] N. Hogan, "Impedance control: An approach to manipulation," in *1984 American Control Conference*. IEEE, pp. 304–313.

[9] O. Khatib, "A unified approach for motion and force control of robot manipulators: The operational space formulation," vol. 3, no. 1, pp. 43–53.

[10] D. Chen, K. Li, X. Jiang, and Y. Liu, "Development of macro-micro robot with a compliant end effector for putty applying," in *2020 IEEE International Conference on Real-time Computing and Robotics (RCAR)*. IEEE, pp. 193–198.